



Dynamic simulation of non-programmed gait generation of quadruped robot

Yuki Takei¹ · Riku Tazawa¹ · Takumi Kaimai¹ · Katsuyuki Morishita¹ · Ken Saito²

Received: 15 April 2021 / Accepted: 28 March 2022 / Published online: 1 June 2022
© International Society of Artificial Life and Robotics (ISAROB) 2022

Abstract

This paper describes a bio-inspired gait generation mechanism for quadruped robots. The gait generation mechanism is an adaptation of one the authors previously developed. Our previous work focused on how a quadruped robot system can generate gaits using pulse-type hardware neuron models (P-HNMs), which have functions similar to the biological neurons. A microcontroller mounted on the robot changed the joints' angle each time the P-HNMs output a pulse. The joints' angular velocity changed by the pulse period's variation according to the toes' pressure. In this paper, the authors imported the previously developed robot's body into a dynamic simulator and implemented the bio-inspired gait generation mechanism. The robot model's mechanical properties are the same as the previously developed robot. The degrees of freedom are excluded except for the legs. Each leg has two joints and a force sensor at the end of the leg. The gait generation mechanism separately controls the legs using each toe's normal force. Instead of using the P-HNMs' pulse period variation, the authors defined a simple mathematical formula in which the joints' angular velocity corresponds to the normal force. The authors confirmed that the robot model could actively generate animals' gaits due to dynamic simulations. The robot model generated the walk gait and the trot gait according to the locomotion speed. These results show that we can generate gaits for quadruped robots by a straightforward method.

Keywords Bio-inspired · Dynamic simulation · Gait generation · Normal force · Quadruped robot

1 Introduction

Legged animals move in situational locomotion. In particular, quadrupeds have a wide variety of locomotion patterns (gaits), and they move efficiently by switching gaits according to their locomotion speed [1–4]. Therefore, implementing the system that generates animals' gaits into robots may let the robots move flexibly and efficiently as animals do.

Neurophysiological experiments have provided insights into the relationships of the nervous systems to gait generation [5–11]. The theory that quadruped animals unconsciously generate gaits by interacting with the central pattern generators (CPGs) and sensory inputs is currently widely accepted [12–14]. Although many neurophysiological experiments, the gait generating mechanisms much remain unknown [15, 16].

Besides neurophysiological studies try to understand animals' complex nervous systems' activity, there are engineering studies. For example, developing models that simulate CPGs and analyzing their behavior have been studied [17–19]. Furthermore, experiments with robot systems using CPG models to generate locomotion have shown advantages such as efficiency, adaptability, and stability [20–24]. However, these results do not necessarily indicate that animals are generating gaits by CPGs of the proposed structures because the structures of animals' CPGs and the function of sensory inputs are unknown.

A study using a biped machine with passive joints revealed that the machine generates a gait placed on a

This work was presented in part at the 26th International Symposium on Artificial Life and Robotics (Online, January 21–23, 2021).

✉ Yuki Takei
csyk19002@g.nihon-u.ac.jp
Ken Saito
saito.ken18@nihon-u.ac.jp

¹ Graduate School of Science and Technology, Nihon University, Tokyo, Japan

² College of Science and Technology, Nihon University, Tokyo, Japan

shallow slope without any joint controlling system [25]. Another study using a quadruped machine showed that it generates quadruped animals' gaits and switches the gait according to the body joints' type and the slope angle [26, 27]. These results suggest even machines that passively move their joints without actively controlling the joints can generate gait using gravity. The finding that walking machines produce different gaits depending on body structure may relate animals' different gaits for different species. Therefore, a gait generation method that appropriately incorporates the body's structure is necessary to apply the animals' gait generation mechanism to engineering.

Quadruped robot systems with active joints controlled by mathematical oscillators demonstrated that they could actively generate gaits. The robot generated gaits according to locomotion speed using toe pressures [28, 29]. The oscillators individually control the joints depending on the oscillators' phases. The pressures accelerate and decelerate the oscillating speed, and it makes phase difference between the legs (i.e., gait) depending on differences in weight supported by each toe. Although they did not design the oscillator they used to control the joint on a biological basis, the suggestion that the toe pressure is closely related to the gait is consistent with the results of physiological experiments [30–32].

The authors attempt to realize a robot that can flexible and efficient walking like animals by implementing a bio-inspired gait generation method. The authors previously developed a quadruped robot system that implemented a gait generation method using pulse-type hardware neuron models (P-HNMs). The P-HNM is an analog circuit that emulates biological neurons' function and can output electrical activity similar to the biological neurons [33]. We demonstrated that the robot system could actively generate the gaits by simply decreasing the joints' angular velocity in response to pressures at the toes [34]. However, the robot system could maintain the gaits only for tens of seconds in the previous experiments. Therefore, we speculate that the cause was the mechanical and electrical disturbance elements and aimed to simulate the robot system in an ideal space to clarify the gait generation's essence.

In this paper, the authors built a quadruped robot model on a dynamic simulator to remove the disturbance elements. Instead of using the P-HNMs' role, we implemented an alternative gait generation method in which the joints' angular velocity corresponds to normal forces.

2 Quadruped robot system

This chapter describes the previously developed quadruped robot system that we based to build a quadruped robot model on the dynamic simulator.

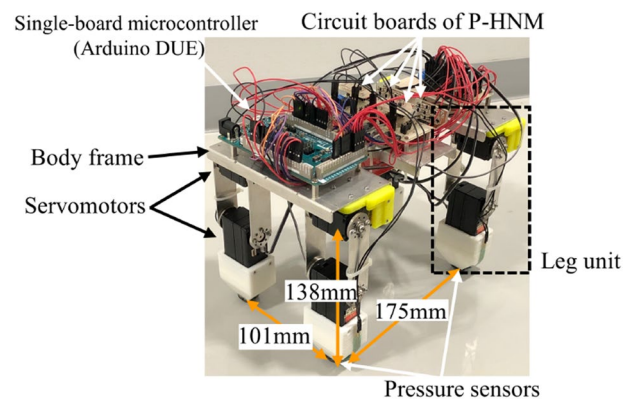


Fig. 1 Quadruped robot system

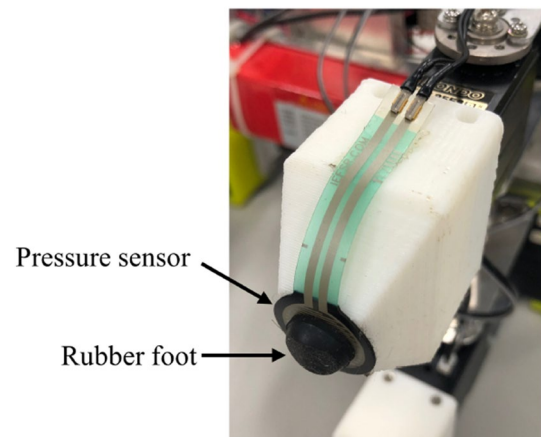


Fig. 2 Detail of leg tip

2.1 Mechanical structure

Figure 1 shows the quadruped robot system. The mechanical components of the robot system are a body frame and four sets of leg units. Every leg units have the same structure with two joints using servomotors each. The robot system has no degrees of freedom except for the leg units. The length from the joints' axis on the body frame side to the toes is 138 mm, the length between the front and rear legs is 175 mm, and the length between the left and right legs is 101 mm. The total weight of the robot system is approximately 1.1 kg. The end of each leg has a pressure sensor and a rubber tip shown in Fig. 2. A single-board microcontroller mounted on the robot system individually controls each leg unit's joints.

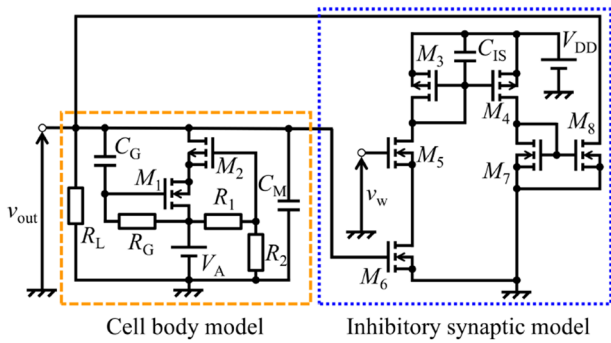


Fig. 3 Schematic diagram of P-HNM

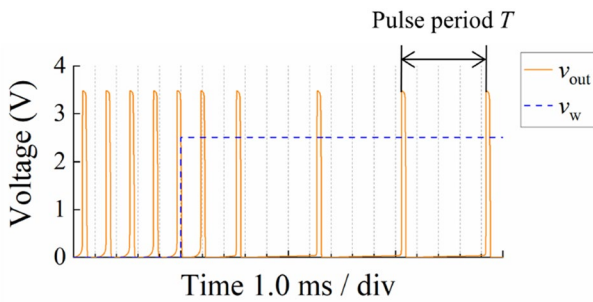


Fig. 4 Example of P-HNM’s output waveform (simulation result)

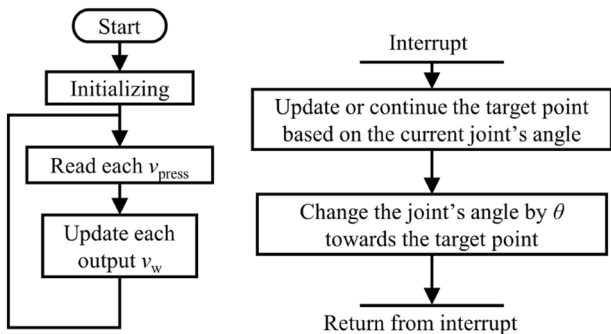
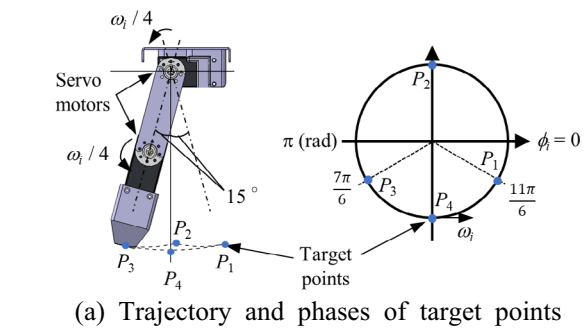


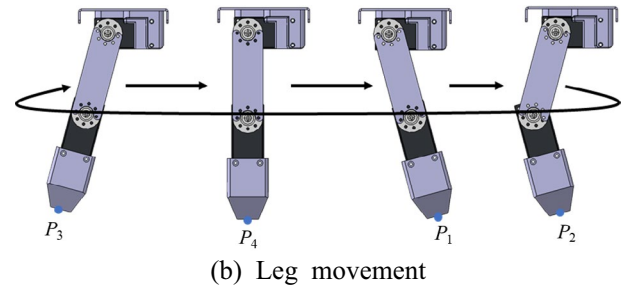
Fig. 5 Summary of microcontroller’s role

2.2 Leg controlling system

The quadruped robot system actively generates gaits by leg controlling systems. The leg controlling system’s components are the microcontroller and the leg unit, the P-HNM, and the pressure sensor. The P-HNM is an analog circuit with functions similar to biological neurons. The P-HNM consists of a cell body model and an inhibitory synaptic model shown in Fig. 3. Details of the cell body model and the inhibitory synaptic model are described in [33]. The P-HNM generates oscillating patterns of electrical activity v_{out} shown in Fig. 4. The synaptic weight control voltage



(a) Trajectory and phases of target points



(b) Leg movement

Fig. 6 Leg movement and trajectory drawn by toes

v_w representing the inhibition’s strength extends the pulse period T .

Figure 5 shows a summary of the microcontroller’s roles. The microcontroller applies the v_w to the P-HNMs depending on each toe pressure. Therefore, the pulse period varies according to their corresponding toe pressure. Each P-HNM inputs the v_{out} to the microcontroller’s different input pin to trigger interrupt commands. When the v_{out} exceeds the interrupt trigger voltage (approximately 1.7 V), the microcontroller runs the corresponding leg’s interruption command. The interruption command changes the angle of joints at a constant angle θ . The toes follow a trajectory shown in Fig. 6a in turn to the target points when changing the angle. ϕ_i in Fig. 6a represents the phase of the leg movements in one cycle. The leg movement when following the target points is as shown in Fig. 6b. For example, if the P-HNM corresponding to the left forefoot triggers an interrupt command, the left forefoot’s joints will move θ toward the next target point. Thus, the quadruped robot system individually varies legs’ moving speed depending on the toe pressure.

2.3 Gait generation method

This section describes the relationship between the pressures and the joints’ angular velocity when the robot locomotes. Since the quadruped robot system controls the leg units individually, parameters are different for each leg. In the following equations, the subscript “ i ” means the parameter for the i th leg. The leg’s angular velocity can be expressed as the following equation:

$$\omega_i = \frac{\theta}{T_i}, \tag{1}$$

where θ is an actuation angle that each time the P-HNM triggers the joints' actuation. θ is a very small value for the angle that the joints need to drive in one cycle of leg motion shown in Fig. 6, and the toes gradually move from a target point to the next target point. The synaptic weight control voltage v_w that the microcontroller applies to the P-HNM circuit boards can be expressed as the following equation:

$$v_{wi} = \sigma v_{pressi} \tag{2}$$

where v_{pressi} is the pressure sensors' output voltages measured by the microcontroller. σ is a constant value for converting v_{press} to v_w and represents the effect of pressure. The period T_i in which the P-HNMs output a pulse can be expressed by the following equation:

$$T_i = 5.0v_{wi}^2 - 8.0v_{wi} + 3.9. \tag{3}$$

From the Eqs. (1) and (3), ω_i is given by the following equation. Equation (4) indicates that the toe's pressure reduces the angular velocity of the joints.

$$\omega_i = \frac{\theta}{5.0v_{wi}^2 - 8.0v_{wi} + 3.9}. \tag{4}$$

This method is based on the method proposed by other researchers to feedback pressure to four decoupled phase oscillators individually [28–30]. In their method, the strength of the feedback to the oscillators varies according to the leg phase. In addition, the feedback accelerates or decelerates the angular velocity according to the leg phase. In contrast, our method does not use the leg phase to vary the angular velocity. Instead, the method feeds back the pressure that the toe receives to the P-HNM to decrease the angular velocity of the joint while not accelerating it.

3 Quadruped robot model

This section describes a quadruped robot model built on the dynamic simulator.

3.1 Modeling

The authors developed a quadruped robot model in the dynamic simulator (CoppeliaSim Coppelia Robotics AG). Figure 7 shows the quadruped robot model. We imported data in STL format we designed to fabricate the quadruped robot system's parts into the dynamic simulator except for a few structures. The parts excluded are mainly

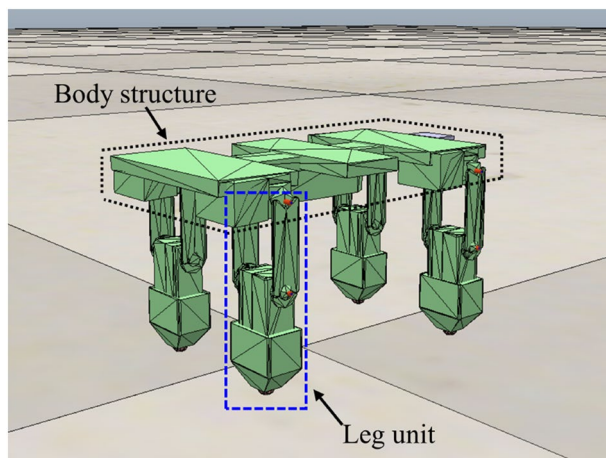


Fig. 7 Quadruped robot model

Table 1 Parts' mechanical parameters

Name	Mass (g)
Body structure	525
Part 1	7.0
Part 2	83
Part 3	1.0
Weight	92

the microcontroller and the circuit boards mounted on the robot's body. Although the data are imported as random non-convex shapes, using them makes the simulations unstable and inaccurate. Therefore, we morphed the imported shapes into stable convex shapes. We set the parts' mechanical properties of the quadruped robot model to the same values as those of the quadruped robot system. Table 1 shows the parts' mechanical properties. The robot model's whole mass is 1.0 kg.

The quadruped robot model consists of a body structure and leg units. Figure 8 shows the structures' detail. The body structure has four joints and a cubic weight to tune the center of mass. Each leg unit has a joint, Part 1, 2, 3, and a force sensor. The leg units have the same structure and mechanical properties. Since the not moving parts can be deemed as a single structure, the body frame and the structure of the servomotors attached to the body frame are merged into a single structure as the body structure for simplicity. Although each Part 1 consists of two structures separated by space, it was also merged into a single structure. All the joints are positioned in the servomotors' axis. We attached the force sensor between Part 2 and 3. The leg modules rotate around the body structure's joints, Part 2, 3, and the force sensors rotate around the leg units' joints together.

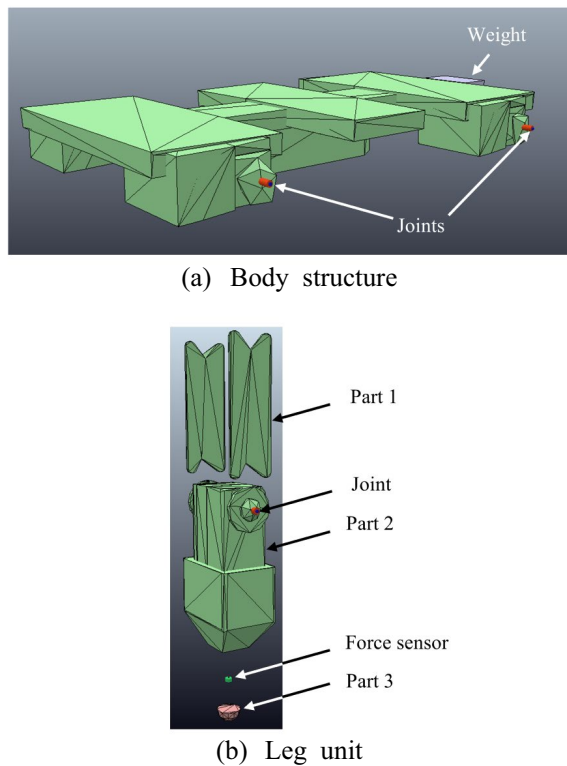


Fig. 8 Detail of body structure and leg unit

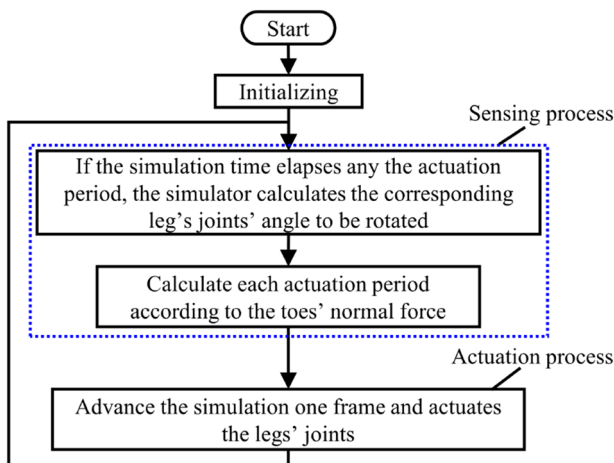


Fig. 9 Summary of simulator's operation

3.2 Alternative gait generation method

We programmed the simulator to control the robot model's legs individually according to the toes' pressures, similar to the quadruped robot system. Figure 9 shows a summary of how the programmed simulator operates. The simulator defines a different joint actuation period for each leg.

Since the simulator defines every actuation period as 0 s in an initializing process, the joints immediately move in an actuation process. A sensing process will start after the initializing process. If the simulation time elapses any the actuation period, the simulator calculates the corresponding leg's joints' angle to be rotated in the actuation process. Then, the simulator calculates each actuation period according to the toes' normal force. After these processes, the simulator advances the simulation one frame and actuates the legs' joints. The time step of the simulations was 10 ms, and the simulator executes the sensing process and the actuation process in every time step. The simulator continues simulation, while the simulation time does not elapse a limit time. Trajectories that the quadruped robot model's toes pass are identical to the quadruped robot system shown in Fig. 6. Target points' phases are also equal. Although the sensors on the toes can measure forces in three axes, we programmed the simulator to use only normal forces to match the quadruped robot system's gait generation method.

The following equations express parameters with primes to distinguish them from the quadruped robot system. Each leg's joint actuation period T' can be expressed as follows:

$$T'_i = T_1 + N_i\sigma', \tag{5}$$

where T_1 is a constant value that corresponds to the P-HNM's pulse period when the normal force is zero in Eq. (3). In other words, Eq. (5) is a simplified quadratic function of Eq. (3) to a linear function. N is the normal force that the toes received from the floor. σ' is a constant value representing the effect of the pressure.

The robot model rotates joints by a constant angle θ' in each actuation period. Therefore, θ' represents the locomotion speed. Hence, the joints' angular velocity ω' is given by the following equation. The weight supported by each leg tip changes the joints' angular velocities, which generates phase differences between the legs.

$$\omega'_i = \frac{\theta'}{T_1 + N_i\sigma'}. \tag{6}$$

4 Dynamic simulation

We simulated the quadruped robot model's behavior in each condition by changing the value of θ' from 0.20° to 1.7° in increments of 0.01° while retaining the constant values T_1 and σ' . The constants we set were $T_1 = 20$ ms and $\sigma' = 8.0$. Each leg's initial phases were $3\pi/2$, and we let the quadruped robot model start moving its legs simultaneously on a wide enough plane. Although we will show transitions of phase differences, the robot model did not recognize and use them to control its legs, as described above.

Fig. 10 Example of generated gait (walk gait)

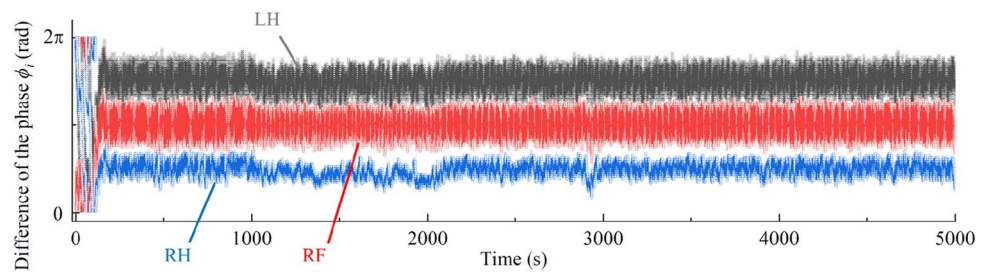
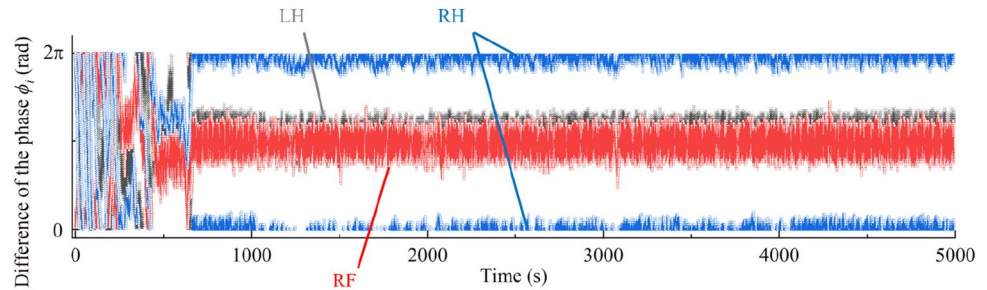
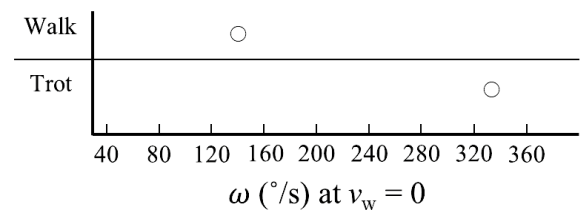


Fig. 11 Example of generated gait (trot gait)

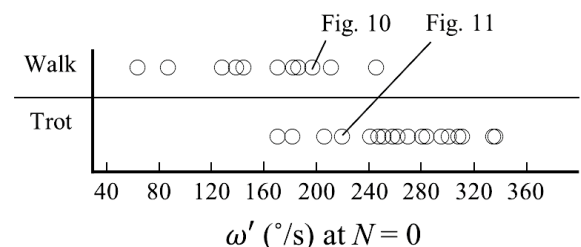


The quadruped robot model actively generated different gait depending on the locomotion speed as the same as the quadruped robot system we have developed. Figures 10 and 11 show examples of how the quadruped robot model generated gaits. These are simulation results in which the quadruped robot model generated each gait most quickly in 5000-s simulations. Also, the results in which the quadruped robot model maintained the gaits for the longest time. The vertical axes in Figs. 10 and 11 represent the difference of the leg movements' phases ϕ_i from the LF (left fore) leg to other legs. The LH, RF, and RH mean left hind, right fore, and right hind leg. The phase differences that the quadruped robot model generated in Fig. 10 are around 90° (0.5π rad). Moreover, the legs' moving order is LF, RH, RF, LH; therefore, this is the walk gait. The θ' in Fig. 10 is 0.99° . The phase differences the robot model generated in Fig. 11 are around 180° (π rad). Furthermore, the legs' moving order is LF and RH, RF and LH; therefore, this is the trot gait. The θ' in Fig. 11 is 1.09° . Our previously developed quadruped robot system could maintain gaits only for tens of seconds. In addition, we could sight the walk gait and trot gait only in two conditions. In contrast, the quadruped robot model could maintain gaits for thousands of seconds.

Figure 12 depicts relationships between angular velocities and generated gaits in simulation and experimental results. Since the variation in angular velocity against pressure is different for the robot system and the robot model, we defined the horizontal axis in Fig. 12 represents angular velocities when a leg tip is not on the floor. The white circles in Fig. 12 indicate conditions in which gaits were maintained for more than five cycles. Figure 12



(a) Experimental results



(b) Simulation results

Fig. 12 Relationships between angular velocities and generated gaits

shows that the robot model could generate each gait in a wide range. Also, Fig. 12 shows that the quadruped robot model tends to generate the walk gait at low speed and the trot gait at high speed.

We speculate that the elimination of disturbances occurred in the robot system, and the simplification of the method caused these differences between the robot system and model.

5 Conclusion

In this paper, the authors described a quadruped robot model with an alternative gait generation method built on a dynamic simulator. We confirmed that the robot model could actively generate animals' gaits due to simulations. The quadruped robot model generated animals' walk gait and trot gait according to locomotion speed. In addition, the robot model could maintain gaits for a much longer cycle than the robot system. The simulation did not faithfully reproduce the robot system. However, since the simplified method could actively generate gaits, it may be close to the essential elements needed for active gait generation.

In the future, we will further analyze the behavior of the quadruped robot model to determine the essential elements.

Acknowledgements This work was supported by Nihon University Multidisciplinary Research Grant for (2020) and supported by Research Institute of Science and Technology Nihon University College of Science and Technology Leading Research Promotion Grant. Also, the part of the work was supported by JSPS KAKENHI Grant number JP18K04060. The authors appreciated the Nihon University Robotics Society (NUROS).

References

- McMahon TA (1985) The role of compliance in mammalian running gaits. *J Exp Biol* 115:263–282
- Yamanobe A, Hiraga A, Kubo K (1992) Relationships between stride frequency, stride length, step length and velocity with asymmetric gaits in the thoroughbred horse. *Jpn J Equine Sci* 3:143–148
- Bhatti Z, Waqas A, Mahesar W, Karbasi M (2017) Gait analysis and biomechanics of quadruped motion for procedural animation and robotic simulation. *Bahria Univ J Inf Commun Technol* 10:2
- Hoyt D, Taylor C (1981) Gait and the energetics of locomotion in horses. *Nature* 292:239–240
- Grillner S (1975) Locomotion in vertebrates: central mechanisms and reflex interaction. *Physiol Rev* 55(2):247–304
- Duysens J (1980) Inhibition of flexor burst generation by loading ankle extensor muscles in walking cats. *Brain Res* 187(2):321–332
- Mori S (1987) Integration of posture and locomotion in acute decerebrate cats and in awake, freely moving cats. *Prog Neurobiol* 28:161–195
- Orsal D, Cabelguen JM, Perret C (1990) Interlimb coordination during fictive locomotion in the thalamic cat. *Exp Brain Res* 82:536–546
- Cruse H, Warnecke H (1991) Coordination of the legs of a slow-walking cat. *Exp Brain Res* 89:147–156
- Rossignol S, Dubuc R, Gossard JP (2006) Dynamic sensorimotor interactions in locomotion. *Physiol Rev* 86:89–154
- Ruber L, Takeoka A, Arber S (2016) Long-distance descending spinal neurons ensure quadrupedal locomotor stability. *Neuron* 92(5):1063–1078
- Grillner S, Zangger P (1979) On the central generation of locomotion in the low spinal cat. *Exp Brain Res* 34:241–261
- Frigon A, Rossignol S (2006) Experiments and models of sensorimotor interaction during locomotion. *Biol Cybern* 95:607–627
- Bellardita C, Kiehn O (2015) Phenotypic characterization of speed-associated gait changes in mice reveals modular organization of locomotor networks. *Curr Biol* 25(11):1426–1436
- Delcomyn F (1980) Neural basis of rhythmic behavior in animals. *Science* 210:492–498
- Arshavsky YI, Deliagina TG, Orlovsky GN (2016) Central pattern generators: mechanisms of operation and their role in controlling automatic movements. *Neurosci Behav Physiol* 46(6):696–718
- Yuasa H, Ito M (1990) Coordination of many oscillators and generation of locomotory patterns. *Biol Cybern* 63:177–184
- Ito S, Yuasa H, Luo Z, Ito M (1998) A mathematical model of adaptive behavior in quadruped locomotion. *Biol Cybern* 78:337–347
- Kukillaya R, Proctor J, Holmes P (2009) Neuromechanical models for insect locomotion: stability, maneuverability, and proprioceptive feedback. *Chaos* 19:1–15
- Ishii T, Masakado S, Ishii K (2004) Locomotion of a quadruped robot using CPG. In: 2004 IEEE International Joint Conference on neural networks 4:3179–3184
- Kimura H, Fukuoka Y, Cohen AH (2007) Adaptive dynamic walking of a quadruped robot on natural ground based on biological concepts. *Int J Robot Res* 26(5):475–490
- Ekeberg Ö, Pearson K (2005) Computer simulation of stepping in the hind legs of the cat: an examination of mechanisms regulating the stance-to-swing transition. *J Neurophysiol* 94(6):4256–4268
- Ijspeert AJ, Crespi A, Ryzcko D, Cabelguen JM (2007) From swimming to walking with a salamander robot driven by a spinal cord model. *Science* 315(5817):1416–1420
- Habu Y, Fukui S, Fukuoka Y (2018) A simple rule for quadrupedal gait transition proposed by a simulated muscle-driven quadruped model with two-level CPGs. In: 2018 IEEE International Conference on robotics and biomimetics (ROBIO), pp 2075–2081
- McGeer T (1990) Passive dynamic walking. *Int J Robot Res* 9(2):62–82
- Nakatani K, Sugimoto Y, Osuka K (2009) Demonstration and analysis of quadrupedal passive dynamic walking. *Adv Robot* 23:483–501
- Sugimoto Y, Yoshioka H, Osuka K (2011) Development of super-multi-legged passive dynamic walking robot “Jenka-III”. In: SICE Annual Conference 2011 pp 576–579
- Owaki D, Kano T, Nagasawa K, Tero A, Ishiguro A (2013) Simple robot suggests physical interlimb communication is essential for quadruped walking. *J R Soc Interface* 10(78):20120669
- Owaki D, Ishiguro A (2017) A quadruped robot exhibiting spontaneous gait transitions from walking to trotting to galloping. *Sci Rep* 7:1–10
- Shinomoto S, Kuramoto Y (1986) Phase Transitions in active rotator systems. *Progress Theoret Phys* 75:1105–1110
- Cartmill M, Lemelin P, Schmitt D (2002) Support polygons and symmetrical gaits in mammals. *Zool J Linn Soc* 136:401–420
- Biancardi CM, Minetti AE (2012) Biomechanical determinants of transverse and rotary gallop in cursorial mammals. *J Exp Biol* 215:4144–4156
- Saito K, Ohara M, Abe M, Kaneko M, Uchikoba F (2017) Gait generation of multilegged robots by using hardware artificial neural networks. In: El-Shahat Adel (ed) Advanced applications for artificial neural networks. IntechOpen
- Takei Y, Morishita K, Tazawa R, Katsuya K, Saito K (2020) Non-programmed gait generation of quadruped robot using pulse-type hardware neuron models. *Artif Life Robot* 26:109–115

Publisher's Note Springer Nature remains neutral with regard to jurisdictional claims in published maps and institutional affiliations.